

NOSE TO BRAIN DELIVERY OF FROVATRIPTAN LOADED IN PLGA NANOPARTICLES: A PROMISING APPROACH FOR MIGRAINE THERAPY

AJEET KUMAR^{1*}, SARAVANAN K¹, SAURABH SHARMA²

¹Department of Pharmacy, Bhagwant University, Ajmer, Rajasthan, India. ²Department of Pharmacy, Vivek University, Bijnor, Uttar Pradesh, India.

*Corresponding author: Ajeet Kumar; Email: ajeet0703bph@gmail.com

Received: 05 June 2025, Revised and Accepted: 25 July 2025

ABSTRACT

Objectives: The objective of the research was to formulate and evaluate frovatriptan succinate (FS)-loaded poly (lactic-co-glycolic acid) (PLGA) nanoparticles (NP) for migraine therapy to improve its therapeutic effect and reduce dosing frequency.

Methods: The objective of the present study was to develop FS-loaded NP for brain targeting to improve bioavailability, decrease dose and frequency of dosing, reduce side effects, and improve therapeutic efficacy. A 3² factorial design was employed to formulate a nanoparticulate drug delivery system using PLGA. PLGA NP were prepared by the nanoprecipitation technique and characterized for particle size, zeta potential, surface morphology, entrapment efficiency (EE), and *in vitro* drug release.

Results: The particle size of the optimized formulation NPopt was found to be 236.1 nm±0.21 nm with EE 63.82±0.643%. Zeta potential was found to be -30.3 mV. Transmission electron microscopy studies indicated that the NPs were spherical with smooth surface. NPopt gave 84.15±1.308% sustained release in phosphate buffered saline pH 6.4 after 24 h, following Quasi-Fickian diffusion-based release mechanism. Stability study showed that the formulation NPopt was more stable at 5±1°C than room temperature. These results showed that FS-loaded PLGA NP can be a potential carrier for brain targeting.

Conclusion: The results suggest that FS-loaded PLGA NP can be a potential carrier for brain targeting with promising therapeutic action.

Keywords: Frovatriptan succinate, Migraine, Nanoparticles, 3² factorial designs, poly (lactic-co-glycolic acid), Nanoprecipitation.

© 2025 The Authors. Published by Innovare Academic Sciences Pvt Ltd. This is an open access article under the CC BY license (<http://creativecommons.org/licenses/by/4.0/>) DOI: <http://dx.doi.org/10.22159/ajpcr.2025v18i10.55432>. Journal homepage: <https://innovareacademics.in/journals/index.php/ajpcr>

INTRODUCTION

The nasal cavity offers appealing routes for drug delivery. Nasal formulations against hypoglycemia and opioid overdose appeared on the market. These medicines are not limited to local action and penetrate either the highly vascularized respiratory mucosa to reach the blood circulation and have systemic effects or the olfactory mucosa to enter the brain directly [1]. Numerous drug delivery systems have been discovered as therapies for brain disorders which may improve efficacy and reduce the toxic effects of the active compounds. The blood-brain barrier (BBB) is the most vital element present in the central nervous system which selectively permits the access of preferred molecules from the blood to the brain. This route exhibits high permeability, bypasses hepatic first pass metabolism, and has a rapid onset of action [2].

The BBB is a semi-permeable barrier with high selectivity. The BBB primarily manages the transport of substances between the blood and the central nervous system (CNS). To enhance drug delivery for CNS disease treatment, various brain-based drug delivery strategies overcoming the BBB have been developed. Nanoparticles (NP) provide targeted therapeutic and diagnostic effects due to higher drug loading and bioavailability, lower dosing frequency, good biocompatibility and biodegradability, greater stability, fewer side effects, and less invasiveness [3]. NPs can be defined as submicron colloidal drug carrier systems which are composed of natural or artificial polymers ranging in size between 10 and 100 nm [4].

NPs have several advantages over other novel delivery systems (microparticles, microemulsions, nano-emulsions, etc.) such as site-specific targeting, prevention of dose dumping through sustained and controlled release, and high surface-to volume ratio. These attributes

indirectly help in reducing dose and frequency of administration which improves patient compliance [5]. The dose size in nasal delivery is limited to 25–200 µL and 25 mg/dose for liquid and powder formulations, respectively, due to the small volume and surface area (160 cm²) of the nasal cavity. Therefore, the nasal route is ideal for potent drugs that require low doses [6,7]. Poly (lactic-co-glycolic acid) (PLGA) is a biodegradable, non-toxic, non-immunogenic, and biocompatibility polymer with ability to encapsulate drugs and also approved as GRAS (Generally Recognized as Safe by the United States Food and Drug Administration) [8].

Migraine is the primary CNS disorder, affecting about 21% of the population. It is characterized by severe headache and pain affecting the one-half part of the brain [9].

Migraine is characterized as a highly prevalent and severely disabling frontotemporal (lasting 4–72 h) pain attack of the head that is commonly associated with nausea and vomiting [10]. Other major symptoms include nausea, vomiting, and sensitivity to light. During the migraine attack, blood vessels of the brain get dilated due to a decrease in the level of the vasoconstrictor known as 5-hydroxytryptamine (5-HT) which causes intense headaches [11]. Other symptoms accompanied with migraine attack are queasiness, phonophobia, and photophobia [12]. Frovatriptan, a second-generation triptan, is 5-HT_{1B} and 5-HT_{1D} receptors agonist prescribed for the management of acute attack of migraine with or without aura. The drug acts by inhibiting excessive dilation of extracerebral and intracranial arteries, thus relieving the pain and other symptoms of migraine headache, that is, nausea, photophobia, and phonophobia. The drug is available in dose of 2.5 mg as conventional tablets given on prescription. The absolute bioavailability of frovatriptan is up to 24% in males and 30% in females

for oral dosage form due to its high first pass metabolism with the poor bioavailability of drug [13]. This route is effective and also evades the problem of dose wastage which may occur due to emesis during a migraine attack. Drug through intranasal route helps in bypassing the BBB, allowing rapid brain localization by direct brain targeting can be achieved with absorption through the olfactory mucosa [14].

Since the treatments available on migraine are old, there is need to develop new acute and preventive therapy for the effective management of migraine disease [15].

The US FDA has adopted a new method called quality by design (QbD). It is a methodical way to make the final product based on specific quality standards called critical quality attributes (CQAs) of the formulation.

We used the QbD approach to study the relationship between formulation parameters (polymers) and CQAs (entrapment efficiency [EE] and particle size) in this study. The goal was to create PLGA NPs as a new drug delivery system for frovatriptan succinate (FS) that could be delivered through the nose to target the brain [16].

MATERIALS AND METHODS

Materials

FS was received as a gift sample from Orchid Chemicals. PLGA obtained from Sigma Aldrich Pvt. Ltd., Mumbai, India. Polyvinyl alcohol (PVA) was obtained from HiMedia, Mumbai. Other chemicals and reagent were obtained from S.D. Fine Chem, India.

Pre-formulation studies

Pre-formulation is the first step in the rational development of dosage form of a drug substance and it is defined as an investigation of physicochemical properties of a drug substance alone and when combined with excipients. Pre-formulation studies are described as the process of optimizing the delivery of drug through the determination of physicochemical properties of the new compound that could affect drug performance and development of an efficacious, stable, and safe dosage form.

λ -Max of FS

The FS standard solution was prepared in phosphate buffer pH 6.8 and scanned using spectrophotometer (Perkin Elmer, Lambda 20). The range for scanning was 200–400 nm. In Fig. 1, the ultraviolet (UV) spectrum of frovatriptan succinate was found to have the working λ -max at 244 nm.

Preparation of standard curve of FS

Accurately weighed 50 mg of FS was dissolved in 50 mL of phosphate buffer pH 6.8 to give a solution of 1,000 $\mu\text{g/mL}$ (Stock Solution I). A 1 mL of this solution was diluted to 100 mL using phosphate buffer pH 6.8 to obtain a solution of 10 $\mu\text{g/mL}$, this solution served as the stock solution II. Into a series of 10 mL volumetric flasks, aliquots of standard solution (i.e., 1, 2, 3, 4, 5, 6, 7, 8, 9, and 10 mL) were added and volume made up to 10 mL using phosphate buffer pH 6.8. The absorbance of these solutions was measured against reagent blank at 244 nm Fig. 2.

Fourier-transform infrared spectroscopy (FT-IR)

FT-IR spectra for pure drug mean detection of the functional groups of drugs by the means of FT-IR spectrophotometer (Shimadzu 4300, Japan) using the KBr disk method [17].

X-ray powder diffraction (XRPD)

X-ray diffraction patterns were measured using the X-ray powder diffractometer (Siemens-850, Germany) using Cu K radiation at a scan rate of 2° min^{-1} over the 2θ range of $5-60^\circ$. XRPD diffraction patterns were determined from the pure drug, polymer, their physical mixture (1:2 and 1:5 ratios), and the resulted NPs [18].

Preparation of FS-loaded PLGA NPs

Selection of method of preparation

Two different methods, namely, as shown in Table 1, emulsification/solvent evaporation (M_1) and nanoprecipitation (M_2), were tried for the preparation of FS-loaded PLGA NPs [19].

Optimization of drug to polymer ratio

Drug-loaded PLGA NPs were as shown in table 2 by nanoprecipitation technique. Accurately weighed 10 mg of PLGA 75:25 (ResomerR-RG752S) and 10 mg drug (1:1) were dissolved in to obtain low viscosity clear solution.

Optimization of surfactant concentration

Accurately weighed 10 mg of drug in ethanol and PLGA 75:25 (ResomerR-RG752S) (30 mg) was dissolved in 10 mL of acetone to obtain low viscosity clear solution. The resulting solution (organic phase) was added slowly to 0.1% w/v PVA aqueous solution, followed by mechanical stirring at 3,000 for 4 h and pulsatile sonication using probe sonicator for 20 min. Similarly, different concentrations of surfactant as revealed in Table 3 were taken, that is, 0.2% w/v, 0.3% w/v, 0.4% w/v, 0.5% w/v, and 1% w/v and, all other parameters were kept constant to obtain the NPs [19].

Optimization of phase ratio (organic/aqueous phase)

Accurately weighed 10 mg of drug in ethanol and PLGA 75:25 (ResomerR-RG752S) (50 mg) (1:5) were dissolved in 10 mL of acetone to obtain low viscosity clear solution. The resulting solution (organic

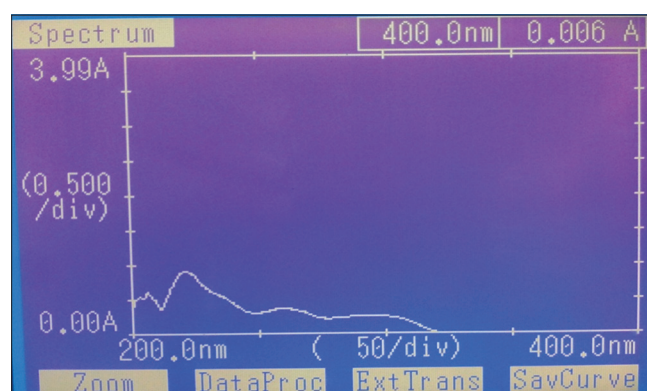


Fig. 1: Ultraviolet spectrum of frovatriptan succinate

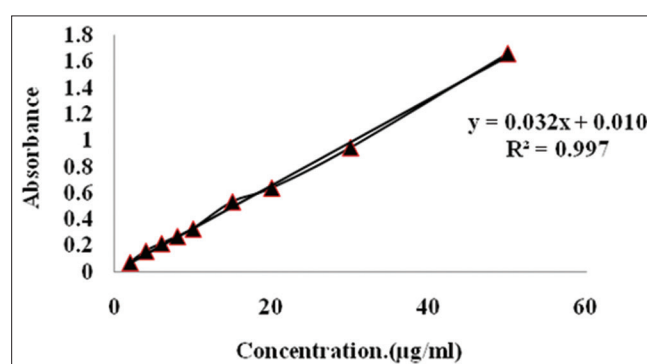


Fig. 2: Regressed curve of frovatriptan succinate

Table 1: Selection of method of preparation

Code	Techniques	Particle size (nm)±SD	Entrapment efficiency±SD
M_1	Emulsification/solvent evaporation method	785±0.75	33.53±0.85
M_2	Nanoprecipitation Method	422±1.23	42.80±0.23

All values are expressed as mean±SD (n=3). SD: Standard deviation

phase) was added slowly to 0.5% w/v PVA aqueous solution, followed by mechanical stirring at 3,000 for 4 h and pulsatile sonication using probe sonicator for 20 min. For optimization, the NPs were prepared with 1:1 to 1:20 (v/v) ratio of organic phase to aqueous phase (Table 4). Phase ratio was optimized with regard to average particle size and %drug entrapment keeping all other parameters constant.

Optimization of sonication time

Accurately weight drug and PLGA (1:5) were dissolved in 10 mL of acetone to obtain low viscosity clear solution. The resulting solution (organic phase) was added slowly to 0.5% w/v PVA aqueous solution, followed by mechanical stirring at 3,000 for 4 h and pulsatile sonication using probe sonicator. Various batches of drug-loaded NP were prepared by varying the sonication time which is listed in (Table 5), that is, 1 min, 5 min, 10 min, and 20 min and keeping all other parameters constant [20,21].

Statistical experimental design for formulation optimization

The design of experiments

Conventionally, pharmaceutical formulations are developed by changing one variable at a time. The method is time-consuming, and it is difficult to evolve an ideal formulation using this classical technique

since the combined effects of the independent variables are not considered. It is therefore important to understand the complexity of pharmaceutical formulations using established statistical tools such as factorial design (FD). FDs, where all the factors are studied in all possible combinations, are considered to be the most efficient in estimating the influence of individual variables and their interactions using minimum experiments. A prior knowledge and understanding of the process and the process variables under investigation are necessary for achieving a more realistic model [22]. The independent variables are controllable, whereas responses are as shown in table 6. Nine batches of NPs were prepared according to a 3^2 full FD, allowing the simultaneous evaluation of two formulation variables and their interaction using Design-Expert®8.0.7.1 trial software [23]. The dependent variables that were selected for study were particle size (Y_1) and % drug entrapment (Y_2). Based on the results and the statistical models as shown in table 7, the software offered optimum setting of formulation for the test conditions [24,25].

Table 8 shows a multiple linear regression model to 3^2 FD which gives a predictor equation incorporating interactive and polynomial term to evaluate the responses:

Table 2: Optimization of drug to polymer ratio

S. No.	Drug to polymer ratio (w/w)	Surfactant concentration (%w/v)	Stirring speed (rpm)	Particle size* (nm) \pm SD	Entrapment efficiency* % \pm SD
1.	1:1	0.5	3,000	-	-
2.	1:3	0.5	3,000	193.6 \pm 0.23	21.70 \pm 0.23
3.	1:5	0.5	3,000	220 \pm 0.91	39.31 \pm 0.12
4.	1:10	0.5	3,000	279.8 \pm 0.02	48.08 \pm 0.61
5.	1:15	0.5	3,000	351 \pm 0.32	46.4 \pm 0.42

All values are expressed as mean \pm SD (n=3). SD: Standard deviation

Table 3: Optimization of surfactant concentration

S. No.	Concentration of PVA % w/v	Drug: Polymer w/w	Particle size* (nm) \pm SD	Polydispersity index (PDI)	Entrapment efficiency* (%) \pm SD
1.	0	1:3	-	-	-
2.	0.1	1:3	418 \pm 0.11	0.197	71.2 \pm 0.65
3.	0.2	1:3	385.1 \pm 0.13	0.501	60.3 \pm 0.54
4.	0.3	1:3	284.6 \pm 0.09	0.215	56.32 \pm 0.13
5.	0.4	1:3	231.8 \pm 0.17	0.310	41.5 \pm 0.18
6.	0.5	1:3	193.6 \pm 0.05	0.287	62.3 \pm 0.87
7.	1	1:3	353.6 \pm 0.18	0.55	49.95 \pm 0.67

All values are expressed as mean \pm SD (n=3). SD: Standard deviation

Table 4: Optimization of phase ratio (organic/aqueous phase)

S. No.	Phase ratio	Drug: Polymer w/w	Concentration of surfactant % w/v	Particle size* (nm) \pm SD	Drug entrapment efficiency* (%) \pm SD
1.	1:1	1:5	0.5	378.4 \pm 0.65	58.9 \pm 0.74
2.	1:5	1:5	0.5	323.1 \pm 0.01	49.98 \pm 0.39
3.	1:10	1:5	0.5	260.8 \pm 0.83	64.21 \pm 0.08
4.	1:15	1:5	0.5	351 \pm 0.34	60.32 \pm 0.92

All values are expressed as mean \pm SD (n=3). SD: Standard deviation

Table 5: Optimization of sonication time

S. No.	Sonication time (min)	Drug: Polymer w/w	Concentration of surfactant % w/v	Particle size (nm) \pm SD	Drug entrapment efficiency (%) \pm SD
1.	1	1:5	0.5	375 \pm 0.56	34.6 \pm 0.45
2.	5	1:5	0.5	351 \pm 0.45	42.4 \pm 0.10
3.	10	1:5	0.5	299.8 \pm 0.89	54.23 \pm 0.04
4.	20	1:5	0.5	222.4 \pm 0.19	63.34 \pm 0.72

All values are expressed as mean \pm SD (n=3). SD: Standard deviation

$$Y = b_0 + b_1X_1 + b_2X_2 + b_3X_1^2 + b_4X_2^2 + b_5X_1X_2 \dots \dots \text{equation}$$

Where Y is dependent variable or response, b_0 is the arithmetic mean response of nine batches, and b_1 estimated coefficient for factor X_1 . The main effects (Y_1 and Y_2) represent average result of changing one factor at a time from its low to high value [26-28].

PLGA NPS characterization

Shape and surface morphology

The morphology of the NPs of the optimized formulation (Nopt) was studied by transmission electron microscopy (TEM) (TECHNAI G 20, 200 KV HR-TEM, FEI Company, Holland). A drop of NPs suspension containing 0.01% of phosphotungstic acid was placed on a carbon film coated on a copper grid for TEM. TEM studies were performed using (TECHNAI G 20, 200 KV HR-TEM, FEI company, Holland). The copper grid was fixed into sample holder and placed in vacuum chamber of the transmission electron microscope under low vacuum, and TEM images were recorded [21].

Particle size analysis

Particle size and size distribution of optimized PLGA NPs formulation was determined by Malvern Zetasizer Ver. 6.01. Each sample was suitably diluted with filtered distilled water (up to 2 mL) to avoid multi-scattering phenomena and placed in a disposable sizing cuvette [17,20].

Zeta potential

Zeta potential was studied to determine the surface charge on the NPs using Malvern Zetasizer (Malvern Instruments, UK). Each sample was suitably diluted 5 times with filtered distilled water and placed in a disposable zeta [29].

TEM

The morphology of NPs in the produced formulations was analyzed using TEM. A droplet of NP suspension containing 0.01% phosphotungstic acid was applied to a carbon layer on a copper grid for TEM. TEM analyses were conducted utilizing the TECHNAI G 20, 200 KV HR-TEM from FEI Company, Netherlands. The copper grid was secured in the sample holder and positioned into the vacuum chamber of the transmission electron microscope under low vacuum, where TEM images were captured [30].

Drug EE

The EE of FS in PLGA NPs was assessed indirectly, determining the free FS (non-entrapped) spectroscopically using UV-VIS Spectrophotometer (Shimadzu) at 244 nm. A fixed quantity of nanosuspension (10 mL) was transferred into a centrifuge tube and centrifuged at 12,000 rpm for 10 min at 20°C (Sartorius F-18K), the absorbance of the free drug in the frovatriptan was determined from the calibration curve [31,32].

$$EE\% = \frac{\text{Total amount of drug} - \text{amount of free drug}}{\text{Total amount of drug}} \times 100\%$$

$$DL\% = \frac{\text{Total amount of drug in nanoparticles}}{\text{Total amount of nanoparticles}} \times 100\%$$

In vitro drug release study

In vitro drug release study was performed using Keshary-Chein (K-C) cell of 25 mL capacity using cellulose acetate membrane (0.2 μ m). The donor compartment contained formulation containing equivalent to 1 mg of drug and receiver compartment was filled with phosphate buffer pH 6.4. The temperature was maintained at $37 \pm 0.5^\circ\text{C}$ with the help of a circulating water jacket. Samples were periodically withdrawn from the receptor compartment, replaced with the same amount of fresh buffer solution, diluted as required with methanol, and analyzed spectrophotometrically at 244 nm [33].

Release kinetics study

In the present study, PLGA NPs were designed for sustained release of NPs for nasal delivery and evaluated for *in vitro* drug release profile in phosphate-buffered saline pH 6.4. The obtained data of the optimized batch were plotted as shown in table 9 as percent drug released versus time (Zero order-equation) Fig. 3, log percentage of drug remaining versus time (first order-equation) Fig. 4, and percentage of drug released versus square root of time (Higuchi's model-equation) Fig. 5 [34,35].

The data obtained from *in vitro* release study were fitted into various kinetic models to determine the release mechanism of FS release from PLGA NPs.

Stability studies

Drug NPs are not stable, which makes them stick together and lose their nanoscale powers. This is one of the main issues with making new medications. How stable the NPs are, and in the end how well the drug delivery system works, will depend on the stabilizer you choose [30].

A study was carried out to assess that the stability of FS-loaded PLGA NPs optimized formulation (NPOpt) were stored in amber colored

Table 6: Experimental range of formulation parameters and critical quality attributes (CQAs) for PLGA nanoparticles

Variables	Levels		
	Low (-1)	Medium (0)	High (+1)
X_1 -Drug polymer ratio	1:3	1:5	1:10
X_2 -Concentration of surfactant (%)	0.1	0.3	0.5
Dependent variables	Constraints		
Y_1 -Particle size (nm)	Minimize		
Y_2 -Entrapment efficiency (%)	Maximize		

PLGA: Poly (lactic-co-glycolic acid)

Table 7: Formulation parameters described in coded level

Batch code	Variables level in coded form		Particle size (nm) (Y_1)	Percentage drug entrapment (Y_2)
	X1	X2		
F1	+1	0	279.8	68.51
F2	0	-1	231.8	48.02
F3	0	+1	351	52.3
F4	+1	-1	236	63.82
F5	0	0	220	50
F6	+1	+1	375	71.06
F7	-1	0	193.6	35.31
F8	-1	+1	299.6	40.09
F9	-1	-1	222.4	29.9

Table 8: Experimental design for 3² factorial design batches

Batch code	Variables level in coded form		Particle size (nm)	Percentage drug entrapment
	X1	X2		
F1	+1	0	279.8	68.51
F2	0	-1	231.8	48.02
F3	0	+1	351	52.3
F4	+1	-1	236	63.82
F5	0	0	220	50
F6	+1	+1	375	71.06
F7	-1	0	193.6	35.31
F8	-1	+1	299.6	40.09
F9	-1	-1	222.4	29.9

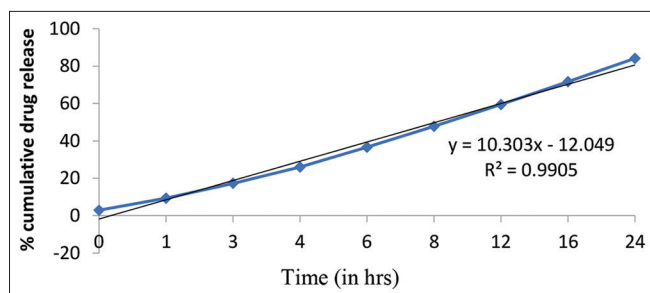


Fig. 3: Plot of zero-order release kinetics of the optimized batch (Nopt) of nanoparticles

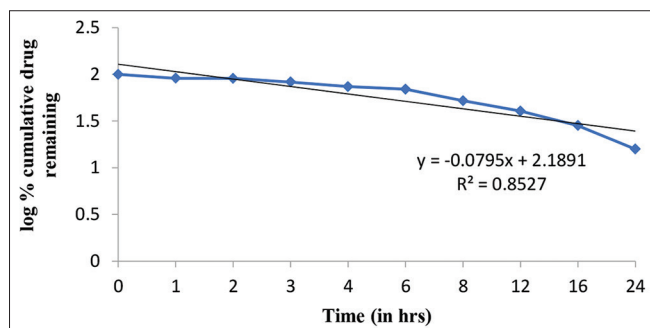


Fig. 4: Plot of first-order release kinetics of the optimized batch (Nopt) of nanoparticles

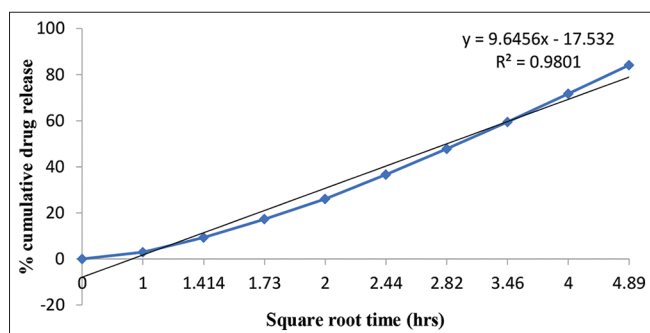


Fig. 5: Plot of Higuchi release kinetics of the optimized batch (Nopt) of nanoparticles

Table 9: Release mechanism with variation in n values

"n" values	Mechanism	dM_t/dt dependence
$N < 0.5$	Quasi-Fickian diffusion	$t^{0.5}$
0.5	Fickian diffusion	$t^{0.5}$
$0.5 < n < 1.0$	Anomalous (non-Fickian) diffusion	t^{n-1}
1	Non-Fickian case II	Zero order
$N > 1.0$	Non-Fickian super case II	t^{n-1}

Table 10: Theta peak comparisons of reference drug and input drug

Compound	Characteristic 2 θ peaks
Reference standard	7.835, 15.767, 16.620, 17.453
Input drug	8.099, 16.033, 16.897, 17.734

Table 11: Summary of results of regression analysis for responses Y1 and Y2

Response	R ²	Adjusted R ²	Predicted R ²	Adequate precision	SD	Percentage CV
Y1	0.9682	0.9365	0.8392	15.273	15.89	5.94
Y2	0.9566	0.9131	0.7801	12.267	4.08	6.95

glass vials at $5 \pm 1^\circ\text{C}$ (Refrigerator) and room temperature. Samples were analyzed for drug content versus time and log % drug content versus time graph as well as any changes in physical appearance of formulation. Samples were analyzed at the intervals of 0, 7, 14, 21, 28, 35, and 45 days [37].

RESULTS

Pre-formulation studies

Pre-formulation testing is the first step in the rational development of dosage forms of a drug substance. It can be defined as an investigation of physical and chemical properties of a drug substance – alone and when combined with excipients. The overall objective of pre-formulation testing is to generate information useful to the formulator in developing stable and bioavailable dosage forms which can be mass-produced.

λ -max of FS

The UV spectrum of FS obtained by scanning the standard drug solution was found to have the working λ_{max} at 244 nm which is shown in Fig. 1.

FT-IR of drug

1 mg of the drug sample and 100 mg of the potassium bromide (KBr) was taken in a mortar and triturated. A small amount of triturated sample was taken into a pellet maker and compressed at 10 kg/cm^2 . The IR spectrum of drug sample was obtained using FTIR-8,400 s, Shimadzu, Figs. 7 and 8 shows important peaks of drug in spectrum.

XRPD

X-ray powder diffraction (XRPD) is defined as an X-ray technique used to analyze powdered crystalline materials, where the resulting diffraction pattern useful for identifying materials based on their unique diffraction patterns as shown in figs. 9-11 and table 10.

Preparation of FS-loaded PLGA NPs

Selection of method of preparation

FS-loaded NPs were prepared by employing two different techniques, namely, emulsification/solvent evaporation method and nanoprecipitation method. In emulsification/solvent evaporation method, the particles were found to be bigger and up to 785 nm with low entrapment $33.53 \pm 0.85\%$. Nanoprecipitation technique was selected as the method of choice in which the formulated particles were of size 422 nm with $42.60 \pm 0.23\%$ drug entrapment.

Two solvents that mix well are needed for nanoprecipitation. In a perfect world, both the polymer and the medicine would dissolve in one solvent but not in the second system, which is the non-solvent. The polymer-containing solvent quickly diffuses into the dispersion medium, causing the polymer to precipitate and trap the medication right away. The Marangoni effect controls the fast creation of NPs. This effect happens at the interface between the solvent and the non-solvent and is caused by complicated and cumulative effects such flow, diffusion, and changes in surface tension.

Optimization of drug to polymer ratio

The impact of polymer concentration was examined utilizing PVA as the surfactant at a concentration of 0.5%. With the augmentation of polymer concentration in the organic phase, specifically at ratios of 1:1, 1:3, 1:5, and 1:10, both particle size and EE exhibited an increase, ranging from 193.6 to 279.8 and 21.70 to 48.01, respectively. The enhancement in EE of FS at elevated polymer concentrations can be attributed to the increased availability of polymer. The increase in particle size can be attributed to enhanced polymer-polymer interactions and the concomitant rise in the viscosity of the aqueous phase, which hinders

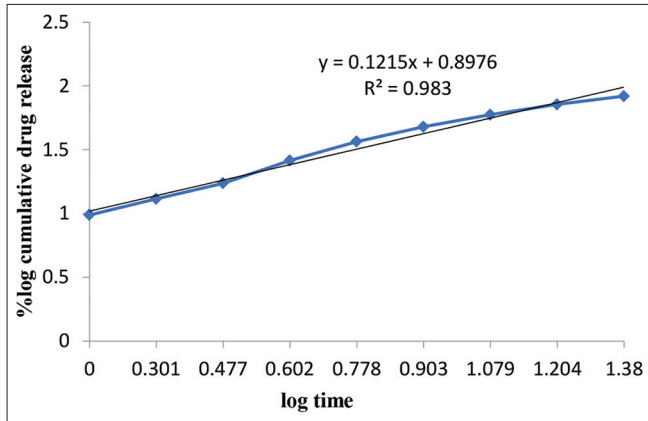


Fig. 6: Plot of Korsmeyer-Peppas release kinetics of the optimized batch (Nopt) of nanoparticles

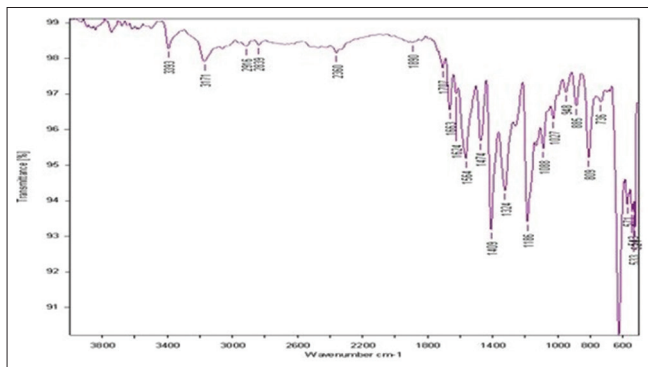


Fig. 7: IR spectrum of frovatriptan succinate

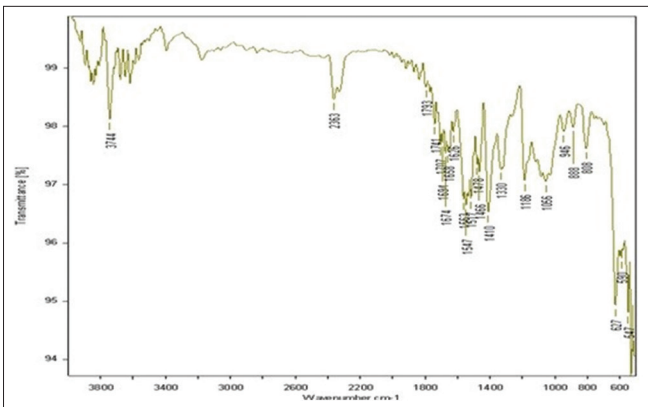


Fig. 8: IR spectrum of drug and polymer taken together

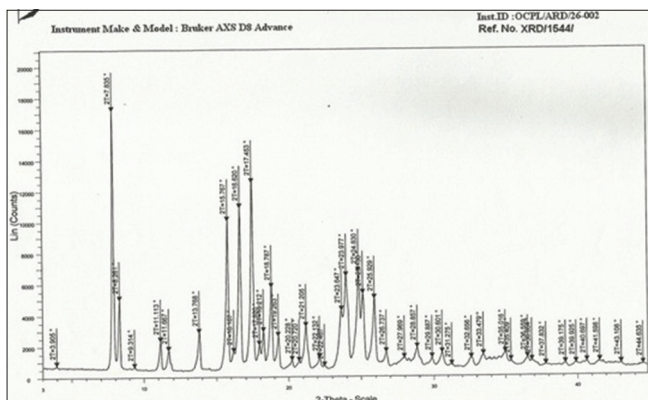


Fig. 9: P-XRD of the reference standard drug

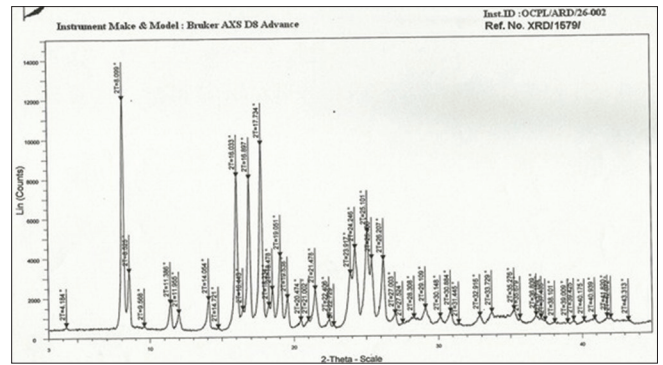


Fig. 10: P-XRD of input drug used for formulation

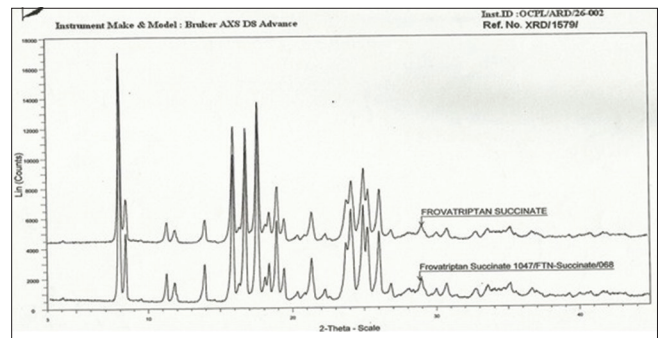


Fig. 11: P-XRD comparison of reference standard and input drug

Table 12: Results of analysis of variance for measured responses

Parameters	DF	SS	MS	F	Significance p
Particle size					
Model	4	30776.35	7694.09	30.48	0.0030
Residual	4	1009.73	252.43	-	-
Total	8	31786.08	7946.52	-	-
Entrapment efficiency					
Model	4	1468.29	367.03	22.02	0.0055
Residual	4	66.69	16.67	-	-
Total	8	1534.98	383.74	-	-

DF indicates degrees of freedom; SS sum of square; MS mean sum of square and F is Fischer's ratio

Table 13: The predicted and observed response variables of the frovatriptan succinate-loaded nanoparticles

Responses	Formulations	Observed value	Prediction value	Prediction error
Y1	F1	193.6	185.8	4.19
	F2	231	222.73	3.71
	F3	299.6	315.67	-5.0
	F4	222.4	234	-4.95
	F5	279.8	273.73	2.21
	F6	375	366.67	2.27
	F7	220	213.40	3.09
	F8	236	248	-4.83
	F9	351	343.27	2.25
Y2	F1	63.50	61.07	3.97
	F2	62.40	59.43	4.99
	F3	71.20	72.63	-1.96
	F4	69.20	71	-2.35
	F5	46.30	44.13	4.91
	F6	68.90	69.9	-1.43
	F7	67.10	68.27	-1.71
	F8	29.9	31.3	4.47
	F9	50.1	48.87	2.51

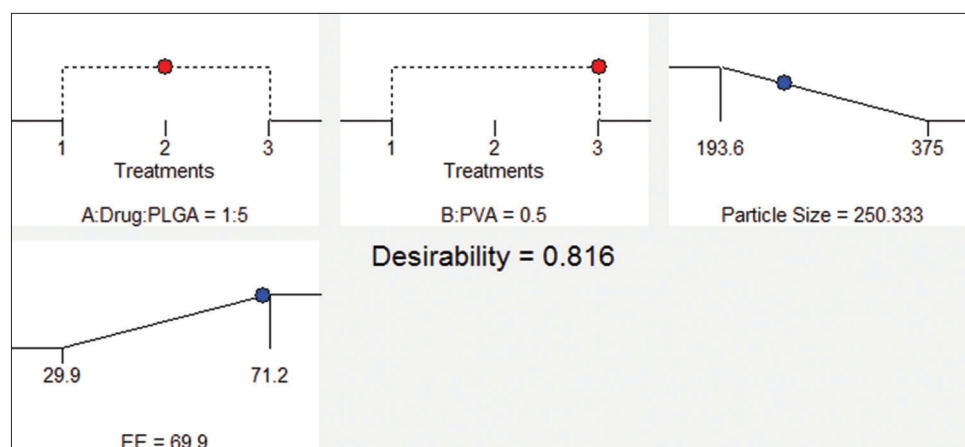


Fig. 12: Predicted factors on the basis of desirability

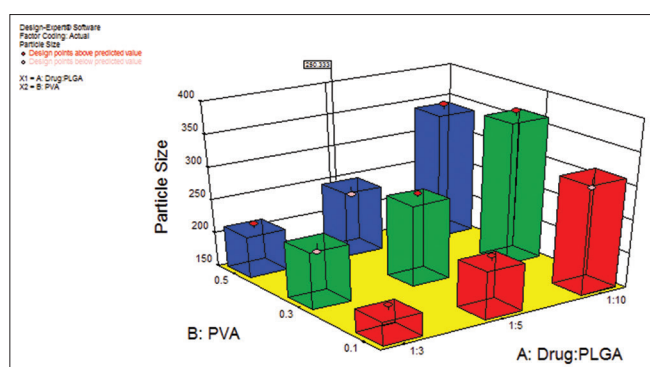


Fig. 13: 3D plot of desired particle size for prediction of optimized batch (Nopt)

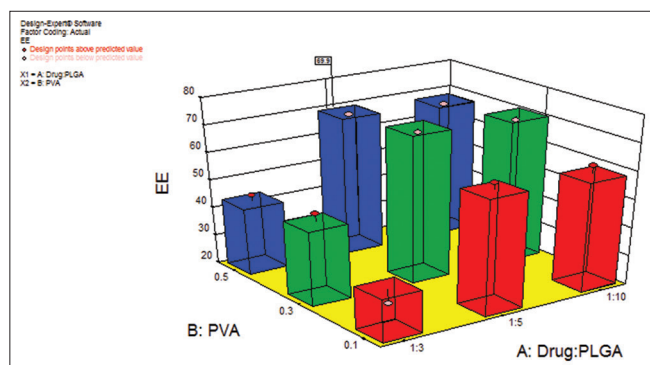


Fig. 14: 3D plot of desired entrapment efficiency for prediction of optimized batch (Nopt)

Table 14: Desired levels of optimization parameter

Two-sided Factor	Name	Level	Confidence=95%		n=1
			Low level	High level	Coding
A	Drug: PLGA	1:5	1:3	1:10	
B	PVA	0.5	0.1	0.5	
Response	Prediction	Standard deviation	SE mean (n=1)	95% PI low	95% PI high
Particle size	250.333	15.8882	11.8423	195.315	305.351
EE	69.9	4.0831	3.04336	55.7609	84.0391

EE: Entrapment efficiency, PLGA: Poly (lactic-co-glycolic acid)

the effective diffusion of solvent into the aqueous phase, resulting in larger particle sizes. Nevertheless, an additional increase in the drug-to-polymer ratio (1:15) resulted in a reduction of drug entrapment in the NPs and an increase in particle size.

Optimization of surfactant concentration

When the NPs suspension was prepared in the absence of surfactant aggregates were observed. To form a proper nanoparticulate suspension, PVA in various concentrations, that is, 0.1%, 0.3, and 0.5% w/v was used. It was found that a decrease in particle size from 418 nm to 193.6 nm was observed as PVA concentration increased from 0.1% to 0.5%. PVA exerts its stabilizing effect by adsorbing at the droplet interface, thus reducing surface tension and promoting mechanical and steric stabilization. Further increase in PVA concentration to 1% led to increase in particle size and was related to increase in viscosity. Particle size increased with decrease in EE when a higher concentration (1% w/v) was used, possibly due to an increase in solubility of the drug in aqueous. At 0.1% PVA concentration, minimum PDI and maximum drug entrapment was observed, at 0.3% w/v PVA concentration, particle size and PDI were found to be in range with 56% drug entrapment and at 0.5% w/v PVA conc. minimum particle size 193 nm was obtained with PDI in range and with 62% drug entrapment as shown in table 15.

Optimization of phase ratio (organic/aqueous phase)

The phase ratio (organic/aqueous phase) was optimized in order to obtain NPs selectively. At phase ratio 1:10 (v/v) of organic phase to aqueous phase, a minimum average particle size 260.8 nm and maximum per cent drug entrapment 64.21% were recorded. On increasing the phase ratio from 1:10 to 1:15 (v/v), an increase in average particle size up to 351 nm was recorded, whereas the percent drug entrapment decreased considerably to 60.32% which may be due to formation of aggregates in the formulation.

Optimization of sonication time

Sonication time was also optimized to achieve stable formulation with minimum average particle size and maximum percent drug entrapment. A stable NP formulation was achieved after sonicating the formulation for 20 min in a pulsatile manner with minimum average particle size of 222.4 nm and maximum percent drug entrapment of 63.34%. A further increase in sonication time (24 min) resulted in an increase in particle size (330 nm) and decrease in percent drug entrapment (59.1%). This may be due to the agglomeration of particles due to generation of surface charge.

Statistical experimental design for formulation optimization

The FD is frequently used for the planning of a research because it provides the maximum amount of information and requires the least number of experiments. Using a 3² FD, the effect of drug to polymer

Table 15: Responses and their derived optimization parameters

Factor	Name	Level	Low Level	High Level	Coding
A	Drug: PLGA	01:05	01:03	01:10	
B	PVA	0.5	0.1	0.5	

99% of population										
Response	Prediction	SD	SE mean	95% CI low	95% CI high	SE pred	95% PI low	95% PI high	95% TI low	95% TI high
Particle size	250.333	15.8882	11.8423	217.454	283.213	19.816	195.315	305.351	127.998	372.668
EE	69.9	4.0831	3.04336	61.4503	78.3497	5.09251	55.7609	84.0391	38.4611	101.339

EE: Entrapment efficiency, CI: Confidence interval, SE: Standard error, SD: Standard deviation, PLGA: Poly (lactic-co-glycolic acid)

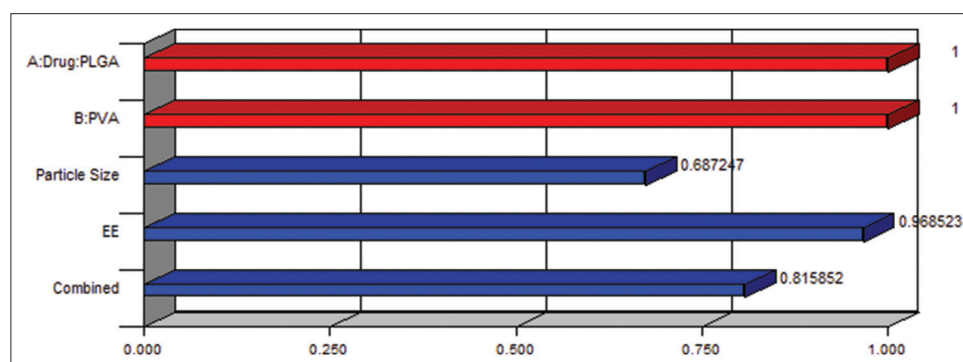


Fig. 15: Bar graph showing individual desirability values of various objective responses and their association overall desirability

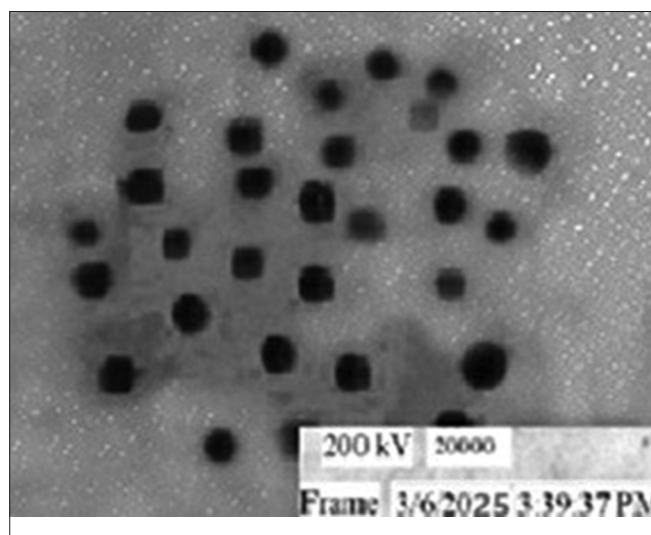


Fig. 16: TEM image of frovatriptan succinate nanoparticles (Nopt)

ratio (X_1) and surfactant concentrations (X_2) on particle size (nm) of NPs (Y_1) and % EE (Y_2) was investigated. A total of nine experiments were performed. The results clearly indicate that all the variables are strongly dependent on the selected independent variables as they show a wide variation among the nine batches its 3D plot and result is shown in figs. 12-15.

To identify the significant effects, statistical analysis of variance (ANOVA) was performed for each parameter. The results of multiple regression analysis are summarized. The particle size and % EE of NPs showed R^2 values of 0.9682 and 0.9566, respectively, for the model. The high values of correlation coefficient (R^2) for the dependent variables indicate a good fit. $p < 0.05$ in the two responses (Y_1 and Y_2) for model terms X_1 and X_2 indicates their significance.

The Model F value of 30.48 in response Y_1 implies that the model is significant. There is only 0.30% chance that a "Model F-Value," this large

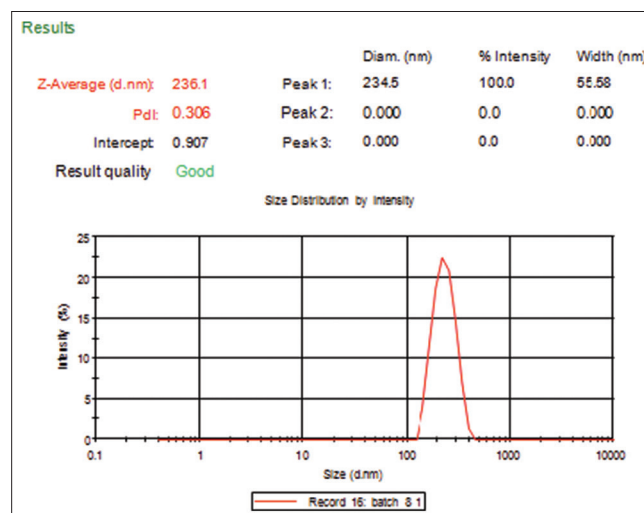


Fig. 17: Particle size of the optimized formulation (Nopt)

could occur due to noise. The Model F value of 22.02 in response Y_2 implies that the model is significant. There is only 0.55% chance that a "Model F- Value" this large could occur due to noise.

"Adeq Precision" measures the signal to noise ratio. A ratio >4 is desirable. An adequate precision value 15.273 and 12.267 suggests the suitability of the model for responses Y_1 and Y_2 , respectively.

To assess the reliability of the model, a comparison between the observed and predicted values of the responses is also presented in terms of % prediction error: It can be seen that in all cases, there was a reasonable agreement between the predicted and the experimental values. This indicates that the optimization technique was appropriate for the FS NPs.

Fitting of data to the model

The two factors with lower, middle, and upper design points encoded and uncoded values are shown in Table 8. The ranges of responses

Y1 and Y2 were 193.6–375 nm and 29.9–71.2%, respectively. All the responses observed for nine formulations prepared were fitted to various models using Design-Expert® software. The values of R^2 , adjusted R^2 , predicted R^2 , SD, and % CV are given in Table 11.

The goodness of fit of the model was checked by the determination of coefficient of regression (R^2). The R^2 value is a measure of total variability explained by the model. In this case, the values of the determination coefficients (R^2) and adjusted determination coefficients (adj R^2) were very high (>90%), which indicates a high significance of the model.

The regression coefficients having $p < 0.05$ are highly significant. The terms having coefficients with $p > 0.05$ are least contributing in the

prediction of particle size and % EE. Values of “Prob >F” <0.0500 indicate that model terms are significant as shown in table 12.

Model F value was assessed by the F statistic, which estimates the percentage of the variability in the outcome.

The low residuals values and the percentage error was <5% hence showed significance of the model used.

Optimization of the formulation using the desirability function

The aim of the optimization of pharmaceutical formulations is generally to find the levels of the variable that affect the chosen responses and determine the levels of the variable from which a robust product with high quality characteristics may be produced as shown in table 13.

Using the desirability function, all the defined responses can be combined into one overall response, the overall desirability as shown in table 14.

PLGA NPS characterization

Shape and surface morphology

Shape and surface morphology of the prepared PLGA NPs was evaluated by TEM. Fig. 16 revealed that the NPs were spherical with a characteristic smooth surface.

Particle size and zeta potential

Particle size and size distribution of prepared PLGA NPs formulation was determined by Malvern Zetasizer Ver. 6.01. The average particle size and polydispersity index (Pdl) of optimized batch (NPopt) was found to be 236.1 nm and 0.306, respectively, as shown in Fig. 17. Pdl is a measure of dispersion homogeneity and usually ranges from 0 to 1. Values close to indicate a homogeneous dispersion while those >0.3 indicate high heterogeneity as shown in table 16.

Zeta potential measurements

In general, greater the zeta potential value of a nanoparticulate system better is the colloidal suspension stability due to repulsion effect between charged NPs. Fig. 18 shows the zeta potential of optimized batch (NPopt) of NPs which were found to be -30.3 mV.

Drug EE

The results of drug EE is given. Percent drug entrapment was found to be 29.941 ± 0.752 to $71.206 \pm 1.347\%$. The EE of optimized batch (NPopt) was found to be 63.82 ± 0.643 .

In vitro drug release study

Fig. 19 shows the *in vitro* drug release profile. The optimized batch showed sustained release of 84.15 ± 1.308 up to 24 h.

Release kinetics

It was found that the *in vitro* drug release of NPopt was best explained by zero order, as the plots showed the highest linearity ($R^2 = 0.990$), followed by Higuchi's equation ($R^2 = 0.980$) and first order, ($R^2 = 0.852$). The corresponding plot (log % cumulative drug release vs. log time) for the Korsmeyer-Peppas equation indicated good linearity as shown in figure 6 ($R^2 = 0.983$). The release exponent “n” was found to be 0.121, which appears (Table 17) to indicate the Quasi-Fickian diffusion.

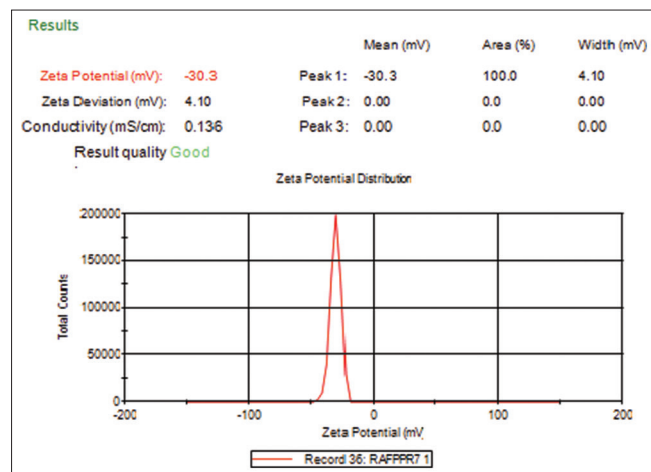


Fig. 18: Zeta potential of optimized formulation (NPopt)

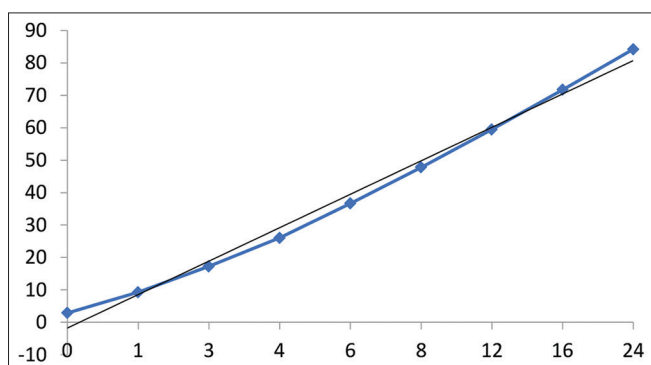


Fig. 19: Plot showing *in vitro* release of Frovatriptan Succinate from the poly (lactic-co-glycolic acid) nanoparticles (NPopt)

Table 16: Parameters of optimized formulation

Formulation	Predicted value		Observed value	
	Particle size	Percentage drug entrapment	Particle size	Percentage drug entrapment
NPopt	250.333	69.9	236	63.82

Table 17: Release parameters of PLGA nanoparticles (NPopt)

Formulation	Zero order		First order		Higuchi		Korsmeyer-Peppas	
	k	R^2	K	R^2	k	R^2	N	R^2
NPopt	10.30	0.990	-0.079	0.852	9.645	0.980	0.121	0.983

PLGA: Poly (lactic-co-glycolic acid)

Table 18: Stability studies (NPopt)

S. No.	Sampling interval (days)	Drug content (%)		Physical appearance	
		5±1°C	Room temperature	5±1°C	Room temperature
1.	0 th	100	100	+	+
2.	7 th	99.53±0.21	99.47±0.22	+	+
3.	14 th	99.35±0.07	97.84±0.15	+	+
4.	21 th	99.19±0.84	97.40±0.08	+	+
5.	28 th	98.85±0.12	97.10±0.17	+	+
6.	35 th	98.53±0.12	96.50±0.12	+	+
7.	45 th	97.19±0.03	96.09±0.34	+	+

(*) Mean±SD (n=3), (+) No change. SD: Standard deviation

Stability studies

Stability was determined by evaluating the percentage of the initial concentration remaining at each time point. Physical appearance was also noted at each time point and optimized batch (NPopt) result shown in table 18.

DISCUSSION

This study developed and tested migraine-treating intranasal PLGA NPs of frovatriptan succinate. Polymeric NP systems sustain therapeutic action and specifically target sites. PLGA is a popular biodegradable and biocompatible polymer. Intranasal medication delivery reduces systemic exposure and increases brain delivery. Drugs are delivered to the brain intranasally. Drugs are delivered to the brain through the olfactory route (bypassing BBB) and blood circulation. Drugs delivered deeply into the nasal cavity use the olfactory pathway to reach the brain. Formulation was optimized using FD. Experiments were designed using Design Expert 8.0.7.1 trial software.

Shape and surface morphology of produced PLGA NPs (NPopt) were assessed by TEM. Most FS NPs were spherical with a smooth surface, according to the study. The average particle size and PDI of NPopt were 231.6 nm and 0.306. NPs have -30.3 zeta potential and 63.82% EE. Stability study was performed according to ICH guidelines and NPopt showed no significant change in the physical appearance at 5±1°C, and room temperature. The K and T_{10%} values for NPopt stored at 5±1°C and room temperature were 1.24×10⁻⁴, 3.79×10⁻⁴, 150, and 105 days, respectively. The T_{10%} obtained in case of formulation stored at 5±1°C was found to be higher as compared with formulation stored at room temperature. Thus, it was concluded that the formulation NPopt is more stable at 5±1°C and tends to degrade faster at higher temperature.

CONCLUSION

It may be concluded on the basis of above discussion that the optimized formulation of FS-loaded PLGA NPs can be successfully prepared by nanoprecipitation technique, and the sets of experiments can be reduced using FD. The prepared NPs displayed good stability during storage. The NPs can be a potential carrier for intranasal delivery for brain targeting.

ACKNOWLEDGMENTS

The author is highly thankful to the Chairman, Department of Pharmaceutical Sciences, for providing necessary facilities.

AUTHORS' CONTRIBUTIONS

Ajeet Kumar: Conceptualized the project, data collection developed the methodology, and drafted the manuscript. Dr. K. Saravanan and Dr. Saurabh Sharma: Reviewed the manuscript, and provided supervision.

COMPETING INTERESTS

The authors declare no conflicts of interest.

FUNDING

None.

REFERENCES

- Rigaut C, Deruyver L, Goole J, Lambert P, Haut B. A comprehensive analytical model for predicting drug absorption in the olfactory region: Application to nose-to-brain delivery. *Int J Pharm.* 2025;674:125392. doi: 10.1016/j.ijpharm.2025.125392, PMID 40032234
- Razavi ZS, Razavi FS, Alizadeh SS. Inorganic nanoparticles and blood-brain barrier modulation: Advancing targeted neurological therapies. *Eur J Med Chem.* 2025;287:117357. doi: 10.1016/j.ejmech.2025.117357, PMID 39947054
- Liu J, Wang T, Dong J, Lu Y. The blood-brain barriers: Novel nanocarriers for central nervous system diseases. *J Nanobiotechnology.* 2025;23(1):146. doi: 10.1186/s12951-025-03247-8, PMID 40011926
- Cayero-Otero MD, Perez-Caballero L, Suarez-Pereira I, Hidalgo-Figueroa M, Delgado-Sequera A, Montesinos JM, et al. Venlafaxine-plga nanoparticles provide a fast onset of action in an animal model of depression via nose-to-brain. *Int J Pharm.* 2025;678:125692. doi: 10.1016/j.ijpharm.2025.125692, PMID 40339630
- Razavi ZS, Alizadeh SS, Razavi FS, Souri M, Soltani M. Advancing neurological disorders therapies: Organic nanoparticles as a key to blood-brain barrier penetration. *Int J Pharm.* 2025;670:125186. doi: 10.1016/j.ijpharm.2025.125186, PMID 39788400
- Gänger S, Schindowski K. Tailoring formulations for intranasal nose-to-brain delivery: A review on architecture, physico-chemical characteristics and mucociliary clearance of the nasal olfactory mucosa. *Pharmaceutics.* 2018;10(3):116. doi: 10.3390/pharmaceutics10030116, PMID 30081536
- Giesinger P, Kiss T, Szabó-Révész P, Ambrus R. The development of an *in vitro* horizontal diffusion cell to monitor nasal powder penetration inline. *Pharmaceutics.* 2021;13(6):809. doi: 10.3390/pharmaceutics13060809, PMID 34071664
- Alghareeb S, Asare-Addo K, Conway BR, Adebisi AO. PLGA nanoparticles for nasal drug delivery. *J Drug Deliv Sci Technol.* 2024;95:105564. doi: 10.1016/j.jddst.2024.105564
- Kataria I, Shende P. Nose-to-brain lipid nanocarriers: An active transportation across BBB in migraine management. *Chem Phys Lipids.* 2022;243:105177. doi: 10.1016/j.chemphyslip.2022.105177, PMID 35122739
- Bhyan B, Bhatt DC, Jangra S. Pharmacokinetic study in humans and *in vitro* evaluation of bioenhanced bilayer sublingual films ForThe management of acute migraine. *Int J Appl Pharm.* 2023;15(3):190-9. doi: 10.22159/ijap.2023v15i3.46684
- Villalón CM, Centurión D, Valdivia LF, De Vries P, Saxena PR. Migraine: Pathophysiology, pharmacology, treatment and future trends. *Curr Vasc Pharmacol.* 2003;1(1):71-84. doi: 10.2174/1570161033386826, PMID 15320857
- Singh H, Singla YP, Narang RS, Pandita D, Singh S, Narang JK. Frovatriptan loaded hydroxy propyl methyl cellulose/treated chitosan based composite fast dissolving sublingual films for management of migraine. *J Drug Deliv Sci Technol.* 2018;47:230-9. doi: 10.1016/j.jddst.2018.06.018
- Kelman L. Review of frovatriptan in the treatment of migraine. *Neuropsychiatr Dis Treat.* 2008;4(1):s1871. doi: 10.2147/ndt.s1871, PMID 18728819
- Negro A, Lionetto L, Casolla B, Lala N, Simmaco M, Martelletti P. Pharmacokinetic evaluation of frovatriptan. *Expert Opin Drug Metab Toxicol.* 2011;7(11):1449-58. doi: 10.1517/17425255.2011.622265, PMID 21929465
- Sawant SH, Mujawar A. Antimigraine activity of methanolic extract of *Abroma augusta* L. In laboratory animals. *Int J Pharm Pharm Sci.* 2022;14:54-9. doi: 10.22159/Ijpps.2022v14i11.45810
- Saleh A, Khalifa M, Shawky S, Bani-Ali A, Eassa H. Zolmitriptan intranasal spanlastics for enhanced migraine treatment; Formulation parameters optimized via quality by design approach, *Sci Pharm.* 2021;89:24. doi: 10.3390/scipharm89020024
- Akel H, Ismail R, Katona G, Sabir F, Ambrus R, Csóka I. A comparison study of lipid and polymeric nanoparticles in the nasal delivery of meloxicam: Formulation, characterization, and *in vitro* evaluation. *Int J Pharm.* 2021;604:120724. doi: 10.1016/j.ijpharm.2021.120724, PMID 34023443
- Kurniawan DW, Aini Gumilas NS, Arramel N, Hartati N, Novrial D, Tarwadi N. Preparation, characterization, and toxicity study of *Andropogonis paniculata* ethanol extract poly-lactic-Co-

- glycolic acid (PLGA) nanoparticles in raw 264.7 cells. *Int J Appl Pharm.* 2024;16:78-83. doi: 10.22159/ijap.2024v16i4.50798
19. Albash R, Fahmy AM, Shamsel-Din HA, Ibrahim AB, Bogari HA, Malatani RT, *et al.* Intranasal propranolol hydrochloride-loaded PLGA-lipid hybrid nanoparticles for brain targeting: Optimization and biodistribution study by radiobiological evaluation. *Eur J Pharm Sci.* 2025;208:107061. doi: 10.1016/j.ejps.2025.107061, PMID 40057137
 20. Sreeharsha N, Prasanthi S, Rao GS, Gajula LR, Biradar N, Goudanavar P, *et al.* Formulation optimization of chitosan surface coated solid lipid nanoparticles of griseofulvin: A Box-Behnken design and *in vivo* pharmacokinetic study. *Eur J Pharm Sci.* 2025;204:106951. doi: 10.1016/j.ejps.2024.106951, PMID 39486655
 21. Tezel G, Ulutürk S, Reçber T, Timur SS, Nemutlu E, Esendağlı G, *et al.* Preparation and *in vitro* characterization of memantine HCl loaded PLGA nanoparticles for Alzheimer's disease. *J Drug Deliv Sci Technol.* 2024;100:106142. doi: 10.1016/j.jddst.2024.106142
 22. Phalak SD, Bodke V, Yadav R, Pandav S, Ranaware M. A systematic review on Nano drug delivery system: Solid lipid nanoparticles (SLN). *Int J Curr Pharm Res.* 2024;16:10-20. doi: 10.22159/ijcpr.2024v16i1.4020
 23. Shah P, Sarolia J, Vyas B, Wagh P, Ankur K, Kumar MA. PLGA nanoparticles for nose to brain delivery of clonazepam: Formulation, optimization by 32 factorial design, *in vitro* and *in vivo* evaluation. *Curr Drug Deliv.* 2021;18(6):805-24. doi: 10.2174/1567201817666200708115627, PMID 32640955
 24. Tong GF, Qin N, Sun LW. Development and evaluation of desvenlafaxine loaded PLGA-chitosan nanoparticles for brain delivery. *Saudi Pharm J.* 2017;25(6):844-51. doi: 10.1016/j.jsps.2016.12.003, PMID 28951668
 25. Piazzini V, Landucci E, D'Ambrosio M, Fasiolo LT, Cinci L, Colombo G, *et al.* Chitosan coated human serum albumin nanoparticles: A promising strategy for nose-to-brain drug delivery. *Int J Biol Macromol.* 2019;129:267-80. doi: 10.1016/j.ijbiomac.2019.02.005, PMID 30726749
 26. Öztürk K, Kaplan M, Çalış S. Effects of nanoparticle size, shape, and zeta potential on drug delivery. *Int J Pharm.* 2024;666:124799. doi: 10.1016/j.ijpharm.2024.124799, PMID 39369767
 27. Wilson BK, Prud'homme RK. Nanoparticle size distribution quantification from transmission electron microscopy (TEM) of ruthenium tetroxide-stained polymeric nanoparticles. *J Colloid Interface Sci.* 2021;604:208-20. doi: 10.1016/j.jcis.2021.04.081
 28. Khalbas AH, Albayati TM, Ali NS, Salih IK. Drug loading methods and kinetic release models using of mesoporous silica nanoparticles as a drug delivery system: A review. *S Afr J Chem Eng.* 2024;50:261-80. doi: 10.1016/j.sajce.2024.08.013
 29. Sultana S, Alzahrani N, Alzahrani R, Alshamrani W, Aloufi W, Ali A, *et al.* Stability issues and approaches to stabilised nanoparticles based drug delivery system. *J Drug Target.* 2020;28(5):468-86. doi: 10.1080/1061186X.2020.1722137, PMID 31984810
 30. Dikpati A, Maio VD, Ates E, Greffard K, Bertrand N. Studying the stability of polymer nanoparticles by size exclusion chromatography of radioactive polymers. *J Control Release.* 2024;369:394-403. doi: 10.1016/j.jconrel.2024.03.053, PMID 38556217
 31. Selvamani V. Stability Studies on Nanomaterials Used in Drugs. Netherlands: Elsevier; 2019. p. 425-44. doi: 10.1016/b978-0-12-814031-4.00015-5
 32. Todaro B, Moscardini A, Luin S. Pioglitazone-loaded plga nanoparticles: Towards the most reliable synthesis method. *Int J Mol Sci* 2022;23:2522. doi: 10.3390/ijms23052522
 33. Kunnumakkara AB, Hegde M, Parama D, Girisa S, Kumar A, Daimary, UD. Role of turmeric and curcumin in prevention and treatment of chronic diseases: Lessons learned from clinical trials. *ACS Pharmacol Transl Sci* 2023;6:447-518. doi: 10.1021/acspsci.2c00012
 34. Haasbroek-Pheiffer A, Niekerk SV, der Kooy FV, Cloete T, Steenekamp J, Hamman J. In vitro and ex vivo experimental models for evaluation of intranasal systemic drug delivery as well as direct nose-to-brain drug delivery. *Biopharm Drug Dispos* 2023;44:94-112. doi: 10.1002/bdd.2348